Analytical intercomparison between type I and type II long-pathlength liquid core waveguides for the measurement of chromophoric dissolved organic matter

Sheri A. Floge,[1]* Kathleen R. Hardy,[1] Emmanuel Boss,[2] and Mark L. Wells[2]
[1]School of Marine Sciences, University of Maine, Darling Marine Center, Walpole, ME, USA
[2]School of Marine Sciences, University of Maine, Orono, ME, USA

Abstract

In the past decade, technological advances in optical sensors have facilitated an increased understanding of the relationship between optical characteristics and biogeochemistry of our oceans. In particular, long-pathlength liquid core waveguide cells (LCWs) are being used to "map" chromophoric dissolved organic matter (CDOM), as a biogeochemical tracer, in various coastal and open ocean regions. At present, two LCW cell types are used in the study of marine CDOM, and concerns about discrepancies in data collected with the different cell types and problems with baseline offsets have arisen. We conducted a direct comparison of absorption coefficient spectra of a dissolved spectrophotometric standard, molecular weight standard (MWS), and dilution series of natural seawater obtained in type I and type II LCWs to assess data agreement and potential colloid-mediated biases. Although no statistical difference was observed for the dissolved standard, we found the type I to have a slight bias toward higher absorption coefficient values for MWS 14–150 kDa (within 95% confidence interval) and natural seawater. Seawater CDOM spectral slopes differed significantly between type I and type II LCWs, with a maximum difference in slope of 0.0006 nm^{-1}. Fastidious elimination of microbubbles from the capillary cells greatly reduced baseline offsets and markedly improved CDOM spectral slope precision.

Introduction

Chromophoric dissolved organic matter (CDOM) is ubiquitous throughout the marine environment and plays a key role in carbon cycling and biogeochemical processes (Blough and Del Vecchio 2002 and references within; Coble 2007 and references within). The exact composition of CDOM likely varies widely but remains largely unknown, therefore CDOM is operationally defined as the pool of organic substances that absorb ultraviolet (UV) or visible light and pass through a filter typically of 0.2 μm pore size (Jerlov 1976). CDOM has an approximately exponential increase in absorption coefficient with decreasing wavelength of radiation and absorbs strongly in the UV and blue visible portion of the spectrum (Bricaud et al. 1981; Blough and Green 1995). As a consequence, CDOM concentrations and spectral signatures can affect ocean color. Recent work has shown the potential use of CDOM as a tracer of water circulation processes (Coble et al. 1998; Blough and Del Vecchio 2002; Nelson et al. 2007; Boehme, J. and M.L. Wells, unpublished observations), and correlation between CDOM and ecological processes (Nelson et al. 1998, 2004; Coble et al. 2004 and references within; Steinberg et al. 2004).

In the past, the study of CDOM dynamics in aquatic environments was hindered by a lack of highly sensitive and portable optical systems capable of detecting CDOM in oligotrophic environments. The standard method for determining CDOM absorption coefficient spectra used conventional spectrophotometers equipped with a 10-cm quartz cell to measure the optical density of filtered seawater samples relative to purified fresh water (Green and Blough 1994; Vodacek et al. 1997) or a 25-cm-pathlength in situ spectrophotometer (WETLabs, ac-9; e.g., Twardowski et al. 1999). The detection limits of most laboratory spectrophotometers equipped with 10-cm cells are insufficient to measure low concentrations of CDOM present in many shelf and open-ocean waters (Miller et al. 2002; Nelson and Siegel 2002). Extraction and concentration of CDOM from natural waters had been used to overcome

problems associated with low concentrations of CDOM (Carder et al. 1989; Green and Blough 1994). However, these methods suffered from problems associated with sample handling (concentration and dilution) and preferential concentration of components of the CDOM pool rather than the entire suite of CDOM present in aquatic systems. Indeed, Green and Blough (1994) found that the absorption coefficient spectra of CDOM isolated via solid-phase C_{18} extraction differed greatly from that found in the original water sample.

One method of increasing spectroscopic sensitivity is to increase the sample cell pathlength via custom long-path cells (Bricaud et al. 1981; Peacock et al. 1994) or capillary optical waveguide cuvettes (D'Sa et al. 1999; Belz et al. 1999; Dallas and Dasgupta 2004). Long-pathlength liquid core waveguides (LCW), introduced commercially by World Precision Instruments in 1997, can be used for high-sensitivity UV-visible absorbance measurements of CDOM. These systems provide optical pathlengths up to tens of meters and require low sample volumes (e.g., 100 µL to 10 mL) (Miller et al. 2002). In a LCW, the sample solution functions as the core of a fluid-filled light waveguide. Light is confined within the liquid core by total internal reflection at or near the cell wall when the refractive index (*n*) of the liquid is higher than the refractive index of the cell wall or covering (Fig. 1) (Belz et al. 1999; D'Sa et al. 1999; Byrne and Kaltenbacher 2001). There are two types of liquid core waveguides (types I and II), which differ solely in the composition of cell wall material. Type I LCW cells consist of solid Teflon AF tubing with a refractive index between 1.29 and 1.31. Type II LCW cells are composed of a fused silica capillary tubing (*n* = 1.46) with an external Teflon AF coating (*n* = 1.29–1.31) (Belz et al. 1999; D'Sa and Steward 2001; Byrne and Kaltenbacher 2001). Light is transported between the waveguide cell and the spectrophotometer via optical fibers.

In recent years, the use of long-pathlength LCWs has facilitated the collection of hyperspectral CDOM absorption coefficient data from open-ocean environments where CDOM detection was not possible by standard methods (Nelson et al. 2007). Additionally, long-pathlength LCWs are being incorporated into various autonomous underwater vehicles and fixed oceanographic observation platforms for the purpose of developing comprehensive CDOM maps (Kirkpatrick et al. 2003). However, there have been reports of discrepancies between absorption coefficient spectra obtained with type II capillary waveguides and conventional spectrophotometers (D'Sa et al. 1999). It has also been suggested that type I and type II LCWs differ significantly in their waveguiding characteristics (Byrne and Kaltenbacher 2001). At present, both cell types are used to generate CDOM absorption coefficient and slope data in diverse natural environments, but it is currently unclear whether data generated with each type are comparable (e.g., Kirkpatrick et al. 2003, Miller et al. 2002).

Spectrophotometric determination of CDOM absorbance involves the measurement of the transmittance of light from the source to the detector through the sample solution. The
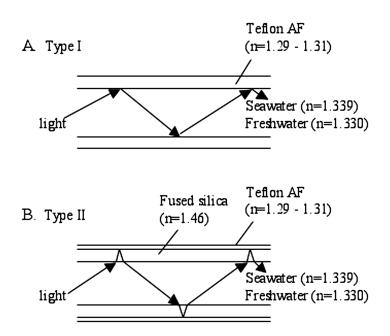

Fig. 1. Cross-sectional view showing light transmission in LCWs. (A) Type I LCW constructed with Teflon AF tubing. (B) Type II LCW constructed with fused silica capillary tubing with a Teflon AF outer coating. The refractive indices of Teflon AF, fused silica tubing, seawater, and freshwater are shown (modified from D'Sa et al. 1999; D'Sa and Steward 2001). This figure is accurate for angles larger than the critical angle for total internal reflection (e.g., when $n_{liquid} > n_{cell\ wall}$ and no scattering agents are present).

light that is lost (beam attenuation) is assumed to be proportional to the absorbance of the CDOM in the sample (absorbance = -log (transmittance)). In reality, beam attenuation is proportional to the amount of light absorbed plus the amount of light scattered. The effect of scattering is generally assumed to be negligible in CDOM absorbance measurements because particulate matter is removed by filtration (0.22 µm). However, the dissolved component contains colloids in the size range of 1–220 nm diameter. Typical concentrations of colloids (<0.1 to 1 µm diameter) in coastal and open-ocean environments range between 10^{13} and 10^{15} m^{-3} (Koike et al. 1990; Wells and Goldberg 1991). Particles <1 µm do not scatter much light in the forward direction, but they do contribute significantly to backscattering (Arnott and Marston 1988; Kuga and Ishimaru 1989; Morel 1991; Stramski and Kiefer 1991; Mobley 1994; Stramski and Wozniak 2005). In conventional spectrophotometers equipped with 1- and 10-cm cuvettes, most of the scattered light will be lost. In contrast, liquid core waveguides will retain scattered light within the cell, where it may repeatedly interact with particles before eventually reaching the light source or the detector. Scattered light will have an increased probability of being absorbed due to the increased pathlength traveled (path amplification). Based on theoretical considerations, backscattering by particles <1 µm is wavelength-dependent, with the effect being more pronounced at shorter wavelengths. Therefore there is a

possibility that scattering by colloids will cause an increase in absorbance at lower wavelengths, with a resultant increase in the calculated CDOM spectral slope. Because of the high sensitivity of capillary waveguide cells, there is a potential then for the variable abundance and size of colloidal matter in seawater to significantly affect CDOM absorption coefficient measurements and calculated slope values obtained with liquid core waveguides.

We conducted a direct comparison of type I and type II liquid core waveguides to assess the agreement of data collected with the two instruments as well as to determine the effect of colloids on absorption coefficient measurements in LCWs. The absorption coefficient spectra of discrete spectrophotometric standards, molecular weight standards, and a dilution series of seawater samples and artificial seawater solutions were contrasted between the two types of liquid core waveguides. We addressed several problems reported by previous investigators (Belz et al. 1999; D'Sa et al. 1999; Byrne and Kaltenbacher 2001), including the causes of baseline offsets and the effects of these offsets on CDOM slope estimates.

Materials and Procedures

Long-pathlength LCW and spectrophotometer setup—The type I liquid waveguide capillary cell (LWCC-1; WPI Inc.) has a 0.5-m physical pathlength and a 500-µm inner diameter. The type I cell is composed of a low-refractive-index polymer tubing (Teflon AF). The type II liquid capillary cell (LWCC-2; WPI Inc.) has a 0.5-m physical pathlength, a 550-µm inner diameter, and a cell composed of fused silica tubing with an outer coating of low-refractive-index polymer (Teflon AF). Both waveguide cells are coiled and have standard ST fiber optic connectors that attach to external optical fibers. The fiber optic cables were connected to the spectrophotometer via a Cary-50 Fiber Optic Dip Probe Coupler (Varian Inc.). Incident light was provided by a Xenon flash lamp within the Cary-50 spectrophotometer (Varian Inc.). Light is axially introduced into the waveguide via a 1-m-long, 400-µm-diameter fiber optic cable (WPI Inc.), and exiting light (that not absorbed or lost to scattering) is collected by a second identical fiber optic cable and returned to the spectrophotometer for absorbance measurements. The spectral range of the Cary-50 is 190–1100 nm, the spectral resolution is 0.15 nm, and the detection range is 0.0005–3 absorbance units (AU). The effective optical pathlengths of the LWCC-1 and LWCC-2 capillary cells were determined to be 0.4807 m and 0.4837 m, respectively, with a holmium wavelength calibration standard (Sigma-Aldrich Inc.) following the procedure of Belz et al. (1999).

Data acquisition—Spectrophotometric measurements were obtained at 1-nm intervals in the wavelength range of 200 to 700 nm. The Cary-50 is a single-beam spectrophotometer, thus sample spectra must be normalized to a reference spectrum. At the start of each experiment, absorbance spectra of replicate deionized water (Milli-Q; Millipore Corp.) samples were collected until the baseline offsets (apparent optical density at 700 nm) of four consecutive spectra were all less than

the observed instrument noise (0.02 m^{-1}) and consistent with previous deionized water spectra collected with the instrument. Repeated cell-flushing and collection of replicate scans was performed to ensure the cell had been flushed of all cleaning reagents and microbubbles. The final deionized water absorbance spectrum was then saved as a reference spectrum or baseline file and automatically subtracted from all subsequent absorbance spectra obtained with each waveguide for the day. Absorbance spectra artifacts due to cell wall contamination were avoided by measuring the absorbance spectra of fresh deionized water samples between each sample scan. Observed baseline offsets and deviations from the deionized water reference spectrum in excess of 0.02 m^{-1} (observed instrument noise level) prompted cell cleaning and recollection of deionized water reference spectrum.

Holmium samples were stored in acid-washed and Milli-Q–rinsed glass vials with Teflon-lined caps, and all remaining samples were stored in vials washed with RBS-35 detergent (Pierce Inc.) and 10% hydrochloric acid solution and put in a muffle furnace for 4 h at 500°C. Samples were introduced to the capillary cell via a sample injector kit (WPI Inc.) with a peristaltic pump pulling the sample through the cell at a speed of 1 mL min^{-1}. The high sensitivity of liquid core waveguides requires that the capillary cell be devoid of cell wall contaminants and microbubbles to obtain accurate baseline and absorbance spectra. The capillary cell was cleaned by pulling a sequence of laboratory detergent (cleaning solution concentrate; WPI Inc.), high-reagent-grade methanol, 2 M HCl, and Milli-Q water through with the peristaltic pump set on maximum pump speed (i.e., prime).

Holmium wavelength calibration standard (Sigma-Aldrich Inc.) 15% wt/vol in perchloric acid, arrived in a sealed glass ampule and was diluted 100-fold with Milli-Q water. The diluted solutions remained at pH <1, acidic enough to prevent holmium polymerization or precipitation (cloudiness or precipitation was not observed). The standard was stored in an amber glass bottle at room temperature, and samples were run in triplicate on each waveguide type within 2 h. Polystyrene sulfonate molecular weight standards (Polymer Standards Service-USA, Inc.) were placed in deionized water to a concentration of 1 mg mL^{-1} and stored overnight in glass scintillation vials at 4°C to fully disperse. Absorbance spectra were measured in each waveguide on six replicate samples for each standard. Surface seawater samples from the Damariscotta River Estuary, Maine (salinity = 30), were collected in acid-washed glass bottles and kept in the dark. Seawater salinity was measured with a handheld refractometer with a precision of ± 1 psu (Fisher Scientific). Samples were drawn into clean (RBS 35 Detergent; Pierce, Inc.) 60-mL polypropylene syringes and filtered through prerinsed 0.2-µm low protein binding Durapore (PVDF) syringe filters (Millipore Corp.) directly into acid-washed amber glass vials. Filtered seawater samples were diluted 1:1 (50% natural seawater) and 1:3 (25% natural seawater) with Milli-Q water due to difficulty preparing chromophore-free artificial seawater solution

for use in the dilutions. All samples were brought to room temperature before absorbance measurements, and the absorbance spectra of triplicate samples were obtained in each waveguide within 2 h of sample collection. At a later date, artificial seawater (Aquil; Morel et al. 1979, Price et al. 1989) was prepared using Milli-Q water, precombusted NaCl, NaSO$_4$, KCl, and KBr and sterile-filtered CaCl$_2$, MgCl$_2$, and NaHCO$_3$, filtered in the same manner as the seawater samples, diluted with Milli-Q water to a salinity equal to 30 and then diluted 1:1 (50% artificial seawater) and 1:3 (25% artificial seawater) with Milli-Q water. These solutions were used to determine the presence of absorbance biases in the seawater dilution series data due to changes in refractive index between sample and waveguide.

Data corrections—Introduction of air to the capillary cell resulted in large baseline offsets (≤9.5 m^{-1} at 700 nm) and subsequent difficulty in comparing absorption coefficient spectra. Although baseline offsets are generally assumed to be wavelength-independent and are corrected by subtracting a constant from the entire absorbance spectra, this assumption has not been verified, and baseline corrections often result in spectral slope changes. By preventing the introduction of air to the cell, we were able to minimize the occurrence and magnitude of baseline offsets. When large baseline offsets were observed, the cell was flushed with 2M HCl, with the peristaltic pump set on maximum speed, while running an absorbance scan. The pump was stopped once the baseline returned to its original value, and the cell was then flushed with Milli-Q water before measuring sample absorbance spectra. We encountered small baseline offsets (<0.14 m^{-1} at 700 nm) in both the molecular weight standard and seawater dilution series absorption spectra. The two data sets were normalized to absorption coefficients at 700 and 500 nm, respectively, and baseline offsets never exceeded 0.16 m^{-1} at 500 nm for seawater absorption coefficients. Baseline offsets were not observed in the holmium standard data.

The spectral absorption coefficients, $a(\lambda)$ (m^{-1}), were obtained using the relationship $a(\lambda) = 2.303A(\lambda)/L$, where $A(\lambda)$ is the measured absorbance at wavelength λ and L is the effective optical pathlength of the waveguide in meters. CDOM spectra typically fit a wavelength-dependent exponential function with a single slope parameter, S (nm^{-1}), particularly in the wavelength range of 320–700 nm (Nelson et al. 2004), such that $a_{cdom}(\lambda) = a_{cdom}(\lambda_0)e^{-S(\lambda-\lambda_0)}$, where λ_0 is the reference wavelength. We determined the spectral slope, S (nm^{-1}), of seawater samples by fitting a single exponential model to the absorption coefficient spectrum between 300 and 500 nm by the nonlinear least-squares method using the minimization routine *fminsearch* in MATLAB (www.mathworks.com). MATLAB optimization parameters *MaxIter* (maximum number of iterations allowed), *MaxFunEvals* (maximum number of function evaluations allowed), and *TolFun* (termination tolerance on the function value) were set at 4000, 2000, and 10^{-9}, respectively. The cost function used was the sum of the squares of the difference between the fitted

curve and the data. A spectrally flat offset correction was used to improve the model fit to the data; the code used is available at http://misclab.umeoce.maine.edu/software.php. The extent to which the model fit the data was examined for every sample (by plotting the residuals). Seawater CDOM slopes, S (nm^{-1}), were calculated between 300 and 500 nm, the spectral range in which the model best fit those data collected. Uncertainties in the slope parameter were determined based on randomly introducing noise, based on the measured variance of triplicate samples, to the spectra and recalculating the slope. Uncertainties in all cases were less than ±0.0001 nm^{-1}.

Assessment

Holmium wavelength calibration standard experiment—This experiment compared the absorption coefficient spectra of a dissolved standard in the type I and type II liquid core waveguides (Fig. 2). The absorption coefficient spectra of the holmium standard obtained with each waveguide type were not significantly different (as assessed by overlap of data within three standard deviations; i.e., the 95% confidence interval). The root mean square of the difference between the two waveguides for a wavelength range of 240–700 nm was 0.0231 m^{-1}. The difference between the two spectra varied between –0.02 and 0.02 m^{-1} in the wavelength range of 375–700 nm. At wavelengths <350 nm, the difference between the two spectra increased to a maximum of 0.08 m^{-1} at 240
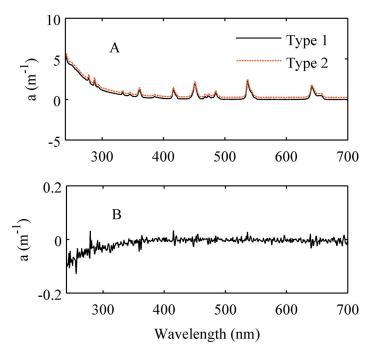

Figure 2. Holmium wavelength calibration standard in type I and type II LCWs. (A) Mean absorption coefficient spectra (n = 3) in type I and type II LCWs. An artificial offset of 0.25 m^{-1} is added to the type II spectra for presentation purposes. (B) Difference between mean absorption coefficient spectra of holmium standard obtained in each waveguide (type I – type II). *X* axes are identical; note different *y* axes.

nm, with a corresponding standard deviation of 0.13 m^{-1}. The holmium standard was used to determine the effective optical pathlengths of the type I and type II waveguides using the method of Belz et al. (1999). This procedure calibrates the pathlength at a single wavelength (536 nm). The agreement of the holmium standard absorption coefficient spectra measured in each waveguide over the spectral range of 240–700 nm indicates that the type I and type II liquid core waveguides do not have wavelength-dependent differences in their measurements of a dissolved standard.

Molecular weight standard experiment—Absorption coefficient measurements were obtained for three molecular weight standards of varying sizes but of equal mass concentration to ascertain whether colloid-mediated scattering occurs within LCWs. We found differences between type I and type II peak absorption coefficients ($\lambda = 262$ nm) of 0.13 ± 0.13 m^{-1}, 0.17 ± 0.07 m^{-1}, and 0.10 ± 0.05 m^{-1} (± 1 SD) for the 14-, 45-, and 150-kDa molecular weight standards, respectively (Fig. 3; Table 1). The root mean square differences between the two cell types in the peak wavelength range of 242–282 nm for the 14-, 45-, and 150-kDa standards were 0.08 m^{-1}, 0.18 m^{-1}, and 0.10 m^{-1}. Absorption coefficients obtained with the type I cell were consistently higher than those found with the type II; however, the differences were within three standard deviations (i.e., the 95% confidence interval) of the replicate scans for each cell type and therefore are not considered significant. Additionally, no significant variations in absorption coefficients among
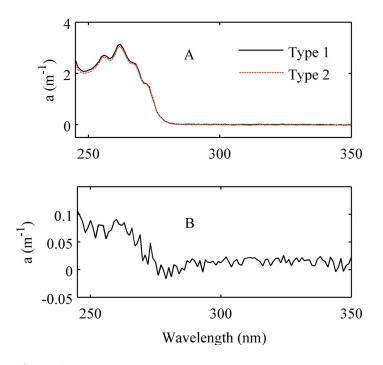
Table 1. Absorption coefficient (262 nm) and corresponding standard deviation of 14-, 45-, and 150-kDa colloidal molecular weight standards in type I and type II LCWs.

MWS, kDa	Type I		Type II	
	a (262 nm; m^{-1})	SD	*a* (262 nm; m^{-1})	SD
14	3.20	0.120	3.07	0.052
45	3.12	0.033	2.95	0.058
150	3.17	0.041	3.07	0.019

molecular weight sizes were found (Table 1). These data suggest that scattering of light within liquid core waveguides due to the presence of colloids is not a problem with particles in the size range of 14–150 kDa. However, since scattering-mediated biases in absorption coefficient measurements will be more noticeable with increasing pathlength, the potential exists for these biases to occur in data collected with longer-pathlength (>0.5 m) LCWs.

The relative amount of backscattered light compared to total scattering increases with decreasing particle size (e.g., Van de Hulst 1981). It is possible that colloid-mediated scattering by particles <14 kDa would result in biases between the two cells and an increase in apparent absorption coefficients at low wavelengths. Indeed, we found significant differences in absorption coefficient values between the LCW types for a 1-kDa molecular weight standard (data not shown). Additionally, the 1-kDa standard exhibited an apparent absorption coefficient approximately twice that of the standards sized 14–150 kDa (data not shown). However, salt concentrations were significantly higher than seawater in this 1-kDa standard, so it is not clear whether the higher absorption coefficient was due to salt effects or colloid backscatter. We were unable to dilute the standard to better delineate the higher absorption coefficient source because the colloid standard suspension is unstable at lower ionic strengths (i.e., the standard forms aggregates of varying size).

Seawater CDOM experiment—A seawater dilution series was used to assess the agreement of natural seawater sample absorption coefficient spectra measured by type I and type II liquid core waveguides and the effect of CDOM concentration on absorption coefficient spectra. (Fig. 4; Table 2). The discrepancy between absorption coefficient measurements via the two cell types increased with decreasing wavelength (or increasing absorption coefficient) with differences at 300 nm equal to 0.27 m^{-1}, 0.14 m^{-1}, and 0.13 m^{-1} for the 100%, 50%, and 25% natural seawater, respectively (Table 2). These differences are approximately equal to 9% of the total absorption coefficient for the 100% and 50% seawater samples and 16% of the total absorption coefficient for the 25% seawater dilution. Absorption coefficient measurements (at 300 nm) made with the type I LCW were significantly higher (as assessed by overlap of data within three standard deviations) for all dilutions than those made with the type II (Table 2). The root

Figure 3. Molecular weight standards in type I and type II LCWs. (A) Mean absorption coefficient spectra of 150-kDa standard (*n* = 6) in type I and type II LCWs. (B) Difference between mean absorption coefficient spectra of 150-kDa standard obtained in each waveguide (type I – type II). *X* axes are identical; note different *y* axes.
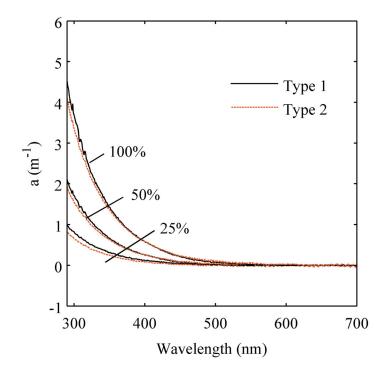
Figure 4. Absorption coefficient spectra of seawater CDOM. Mean absorption coefficient spectra ($n = 3$) of three dilutions of filtered seawater (undiluted, 50%, and 25%) in type I and type II LCWs.
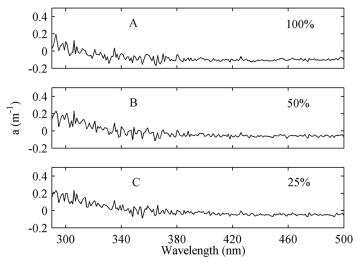

Figure 5. Difference between mean absorption coefficient spectra of undiluted (A) and 50% (B) and 25% (C) dilutions of artificial seawater obtained in each waveguide (type I – type II). *X* and *y* axes are identical.

mean square of the difference (300–500 nm) for 100%, 50%, and 25% natural seawater were 0.09 m^{-1}, 0.05 m^{-1}, and 0.14 m^{-1}, respectively.

Light transmission within LCWs depends on the refractive index of the core solution (D'Sa et al. 1999; Byrne and Kaltenbacher 2001; Miller et al. 2002). Wavelength-dependent offsets resulting from changes in solution salinity have been observed in both type I (Nelson et al. 2007) and type II (M. Belz, personal communication) LCWs. The extent and direction (positive or negative) of the offset is unique to each individual cell (M. Belz, personal communication) thus necessitating correction of the refractive index effect. Absorption coefficient values obtained with the type I cell exhibited a salinity-dependent positive offset (higher absorption coefficient) that increased with decreasing wavelength to 0.24 m^{-1}, 0.18 m^{-1}, and 0.12 m^{-1} at 300 nm for undiluted (100%), 50%, and 25% artificial seawater, respectively. A similar positive offset also was observed in the type II LCW, though to a lesser extent: 0.17 m^{-1}, 0.06 m^{-1}, and ~0 m^{-1}

at 300 nm for undiluted (100%), 50%, and 25% artificial seawater samples, respectively. Even so, there was little difference in absorption coefficients between the two cell types for the three dilutions (Fig. 5) (~0.07 m^{-1}, 0.12 m^{-1}, and 0.12 m^{-1} for undiluted, 50%, and 25%). Although salt-mediated refractive index effects largely explain the absorption coefficient differences between the two LCW types at 50% and 25% dilution, they do not explain the absorption coefficient difference measured for natural seawater (~0.27 m^{-1} at 300 nm for 100% seawater; Table 2).

It appears then that the type I LCW yields higher absorption coefficient values relative to the type II for both the range of molecular weight standards (although not statistically significant) and natural seawater CDOM, whereas no difference was found for the dissolved holmium standard. The implication of our findings is that colloidal backscatter might produce biases among data collected by the two cell types, with the type I LCW being slightly more prone to scattering-mediated light losses than the type II. It is worth noting though that whereas these absorption coefficient differences were larger than the refractive index corrections, a more comprehensive series of correction factors might bring closer agreement among data collected by the two LCW types.

Absorption coefficient spectra obtained for the 100% and 25% seawater CDOM samples with the type I and type II

Table 2. Seawater CDOM absorption coefficient at 300 nm.

Percent of natural seawater	Type I		Type II	
	a (300 nm; m^{-1})	SD	*a* (300 nm; m^{-1})	SD
25	0.82	0.030	0.69	0.000
50	1.70	0.021	1.56	0.007
100	3.66	0.075	3.39	0.005

Mean absorption coefficient ($n = 3$) and corresponding standard deviation.

Table 3. Spectral slopes of seawater CDOM.

	Type I		Type II	
Percent of natural seawater	S (300–500 nm; nm⁻¹)	SD	S (300–500 nm; nm⁻¹)	SD
25	0.0185	0.0002	0.0191	0.0001
50	0.0182	0.0001	0.0181	0.0001
100	0.0185	0.0000	0.0179	0.0001

Mean spectral slope ($n = 3$) and corresponding standard deviation.

waveguides had significantly different slopes (300–500 nm) (as assessed by overlap of data within three standard deviations) (Table 3). The differences in spectral slope values (S) obtained with the two LCW types for the 100%, 50%, and 25% natural seawater samples were 0.0006 nm⁻¹, 0.0001 nm⁻¹, and 0.0006 nm⁻¹. These differences may be due in part to wavelength-dependent absorption coefficient biases caused by refractive index effects and could potentially be reduced through careful indices of refraction matching of sample and reference solution (Miller et al. 2002; Nelson et al. 2007). Alternatively, these differences may be a result of the baseline offset correction used in our spectral fit. The observed differences in spectral slope between the two LCW types are well within typical error values reported in the literature (Twardowski et al. 2004), even without refractive index corrections.

Variations in S with dilution were nonlinear in the type I LCW, with the 100% and 50% natural seawater samples being significantly different from one another (0.0003 nm⁻¹). In contrast, type II LCW measurements resulted in spectral slopes that increased with decreasing salinity (difference of 0.0012 nm⁻¹), with the 25% seawater being significantly different from the 50% and 100% natural seawater samples. Although the cause for increasing S with dilution in the type II LCW is unclear, the data are consistent with previous reports (Kirkpatrick et al. 2003). The high precision of LCW-mediated absorption coefficient scans renders these differences significant (with respect to data overlap within three standard deviations); however, the observed variations with dilution are within typical reported error values (Twardowski et al. 2004).

Discussion

In the past 5 years, a newfound interest in CDOM as a biogeochemical tracer has emerged (Coble et al. 1998, 2004; Nelson et al. 2007). This interest sprang from concurrent advances in both satellite-based estimates of oceanic CDOM and optical instrumentation for in situ CDOM measurements as well as recent indications that changes in open-ocean CDOM signatures reflect local ecological processes (Nelson et al. 1998, 2004; Steinberg et al. 2004). Improvements in satellite instrumentation (McClain et al. 1998) and retrieval algorithms (Roesler and Perry 1995; Garver and Siegel 1997; Maritorina et al. 2002) now enable remote estimates of surface seawater CDOM on a global scale (Siegel et al. 2002), and

long-pathlength liquid core waveguide cells enable CDOM measurements in oligotrophic environments.

The general view held by optical oceanographers over the past several decades was that open-ocean CDOM concentrations are negligible and merely reflect patterns in riverine input (Hojerslev 1982). New satellite-based estimates of global CDOM show that riverine CDOM inputs actually have little impact on open ocean CDOM signatures (Siegel et al. 2002). Additionally, large (>5-fold) seasonal variations in basin CDOM have been observed (Siegel et al. 2002). A host of studies have found that CDOM concentrations and spectral signature vary in response to local production and destruction processes (both biotic and abiotic) (Blough and Del Vecchio 2002 and references within; Nelson and Siegel 2002 and references within; Nelson et al. 2004) and could potentially serve as a biogeochemical tracer in coastal and open-ocean waters.

These recent insights into marine CDOM dynamics have prompted the growing use of LCWs for CDOM measurements in coastal (D'Sa et al. 2002; Miller et al. 2002; Kirkpatrick et al. 2003; Floge and Wells 2007) and open-ocean (Nelson et al. 2007) regions. Indeed, Nelson et al. (2007) used a type I cell (Ultrapath; WPI Inc.) to map CDOM distributions in the North Atlantic Ocean, whereas type II LCW cells are being incorporated into various autonomous in situ optical sensors (Kirkpatrick et al. 2003). Unfortunately, concerns have been raised about wavelength-dependent biases and lack of compatibility in data collected with the two LCW cell types (D'Sa et al. 1999).

Our study results show that data obtained with type I and type II LCWs have statistically significant differences in seawater CDOM absorption coefficient and spectral slope values. The positive offset in seawater CDOM absorption coefficient data collected in the type I compared to the type II is not likely to be of consequence in coastal waters, where CDOM absorption coefficients are relatively high [e.g. a(400 nm) up to 30 m⁻¹; Miller et al. 2002]. However, comparison of absorption coefficient intensity data between the two cell types will be difficult among open-ocean CDOM studies, where average CDOM absorption coefficient ranges from 0.05 to 0.15 m⁻¹ (at 325 nm) (Nelson et al. 2007).

D'Sa et al. (1999) stated that the estimation of CDOM slopes with liquid core waveguide absorption coefficient measurements would be difficult until baseline offsets were minimized. They attributed baseline offsets to differences in the

refractive index between samples and reference solutions and suggested that baseline offsets could be minimized through careful matching of the refractive indexes of solutions. At the start of our experiments, we observed baseline offsets of up to 9.5 m^{-1} in each of the waveguide types that greatly impacted the precision of slope estimates (SD >0.001 m^{-1}). Our observations of large baseline offsets in replicates of deionized (Milli-Q) water samples suggested that the offsets were due to something other than differences in refractive indices, and our experiments indicated that these offsets instead were attributable to microbubbles within the capillary cells. Potential sources of bubble introduction and formation within the LWCC cell include incomplete seal between sample injector piece and LWCC injection port, direct syringe-injection of sample, warming of samples initially less than room temperature and drawing non-predegassed samples through the cell. Both type I and type II liquid core waveguides are capable of producing high-precision absorption coefficient measurements on replicate samples if the cell wall is kept free of contaminants and the introduction and formation of microbubbles to and within the cell are avoided.

The slope of CDOM is used to provide information about the nature of CDOM chromophores found in the environment and is believed to vary with the source of the CDOM as well as with biological and chemical transformations of the source material. CDOM slope values found in natural environments range from 0.011 nm^{-1} for freshwater high in humic acid to 0.025 nm^{-1} for open-ocean waters (Blough and Del Vecchio 2002). Calculated CDOM slopes have been reported in the literature with standard deviations ranging from 0.001 to 0.03 nm^{-1} (Twardowski et al. 2004). Our data showed a maximum difference in slopes between the type I and type II waveguide to be 0.0006 nm^{-1}. The small magnitude of this difference indicates that spectral slopes are comparable between the two cell types.

Ocean color is becoming widely recognized as a valuable tool for the study of both coastal and open-ocean environments. Hyperspectral measurements provide information on the composition and concentration of dissolved and particulate materials in seawater, facilitating new insights into ocean biogeochemistry and mixing dynamics as well as being used for water quality monitoring and management. Until recently, open-ocean color dynamics and the ecological and physical processes associated with these dynamics were concealed due to low CDOM detection limits. The advent of long-pathlength liquid core waveguides has enabled unprecedented measurements of CDOM in oligotrophic environments. Our findings indicate that the potential exists for colloid-mediated scattering within LWCCs to cause absorption coefficient biases between the two cells and among samples of varying colloidal abundance and size distribution. However, the biases observed here were of such small magnitude that we conclude that with careful avoidance of microbubbles and consequent baseline

offsets, and application of comprehensive refractive index corrections, highly precise and comparable ocean color absorption coefficient measurements may be obtained with either LWCC cell type for coastal waters. Whereas open-ocean absorption coefficient values may be significantly affected by differences due to cell type, spectral slopes appear to be directly comparable between the two instruments for both high- and low-absorbing waters.

References

Arnott, W. P., and P. L. Marston. 1988. Optical glory of small freely rising gas bubbles in water: observed and computed cross-polarized backscattering patterns. J. Opt. Soc. Am. A. 5:496.

Belz, M., P. Dress, A. Sukhitskiy, and S. Liu. 1999. Linearity and effective optical pathlength of liquid waveguide capillary cells. SPIE. 3865:271-281.

Blough, N. V., and R. Del Vecchio. 2002. Chromophoric DOM in the coastal environment. *In* D. A. Hansell and C. A. Carlson [eds.], Biogeochemistry of Marine Dissolved Organic Matter. New York: Academic, p. 509-546.

——— and S. A. Green (1995) Spectroscopic characterization and remote sensing of non-living organic matter. *In* R.G. Zepp and C. Sonntag [eds.], The Role of Nonliving Organic Matter in the Earth's Carbon Cycle. New York: Wiley, p. 23-45.

Bricaud, A., A. Morel, and L. Prieur. 1981. Absorption by dissolved organic matter of the sea (yellow substance) in the UV and visible domains. Limnol. Oceanogr. 26:43-53.

Byrne, R. H., and E. Kaltenbacher. 2001. Use of liquid core waveguides for long pathlength absorbance spectroscopy: principles and practice. Limnol. Oceanogr. 46:740-742.

Carder, K. L., R. G. Steward, G. R. Harvey, and P. B. Ortner. 1989. Marine humic and fulvic acids: their effects on remote sensing of chlorophyll. Limnol. Oceanogr. 34:68-81.

Coble, P. G. 2007. Marine optical biogeochemistry: the chemistry of ocean color. Chem. Rev. 107:402-418.

———, C. E. Del Castillo, and B. Avril. 1998. Distribution and optical properties of CDOM in the Arabian Sea during the 1995 Southwest Monsoon. Deep-Sea Res. II. 45:2195-2223.

———, C. Hu, R. W. Gould Jr, G. Chang, and A. M. Wood. 2004. Colored dissolved organic matter in the coastal ocean. Oceanography 17:50-59.

D'Sa, E. J., C. Hu, F. E. Muller-Karger, and K. L. Carder. 2002. Estimation of colored dissolved organic matter and salinity fields in case 2 waters using SeaWIFS: examples from Florida Bay and Florida Shelf. Proc. Indian Acad. Sci. 111:197-207.

———, R. G. Steward, A. Vodaceck, N. V. Blough, and D. Phinney. 1999. Determining optical absorption of colored dissolved organic matter in seawater with a liquid capillary waveguide. Limnol. Oceanogr. 44:1142-1148.

——— and R. G. Steward. 2001. Liquid capillary waveguide application in absorbance spectroscopy. Limnol. Oceanogr. 46:742-745.

Dallas, T., and P. K. Dasgupta. 2004. Light at the end of the tunnel: recent analytical applications of liquid-core waveguides. Trends Anal. Chem. 23:385-392.

Floge, S. A., and M. L. Wells. 2007. Variation in colloidal chromophoric dissolved organic matter in the Damariscotta Estuary, Maine. Limnol. Oceanogr. 52:32-45.

Garver, S. A., and D. A. Siegel. 1997. Inherent optical property inversion of ocean color spectra and its biogeochemical interpretation: I. Time series from the Sargasso Sea. J. Geophys. Res. 102:18607-18625.

Green, S. A., and N. V. Blough. 1994. Optical absorption and fluorescence properties of chromophoric dissolved organic matter in natural waters. Limnol. Oceanogr. 39:1903-1916.

Hojerslev, N. 1982. Yellow substance in the sea. *In* J. Calkins [ed.], The role of solar ultraviolet radiation in marine ecosystems. New York: Plenum, p. 263-281.

Jerlov, N. G. 1976. Marine Optics, 2nd ed. New York: Elsevier.

Kirkpatrick, G. J., C. Orrico, M. A. Moline, M. Oliver, and O. M. Schofield. 2003. Continuous hyperspectral absorption measurements of colored dissolved organic material in aquatic systems. App. Opt. 42:6564-6568.

Koike, I., S. Hara, K. Terauchi, and K. Kogure. 1990. Role of submicrometer particles in the ocean. Nature. 345:242-244.

Kuga, Y., and A. Ishimaru. 1989. Backscattering enhancement by randomly distributed very large particles. Appl. Opt. 28:2165.

Maritorena, S., D. A. Siegel, and A. R. Peterson. 2002. Optimal tuning of a semi-analytical model for global applications. Appl. Opt. 41:2705-2714.

McClain, C. R., M. L. Cleave, G. C. Feldman, W. W. Gregg, S. B. Hooker, and N. Kuring. 1998. Science quality SeaWiFS data for global biosphere research. Sea Technol. 39:10-16.

Miller, R. L., M. Belz, C. Del Castillo, and R. Trzaska. 2002. Determining CDOM absorption spectra in diverse coastal environments using a multiple pathlength, liquid core waveguide system. Cont. Shelf Res. 22:1, 301-1, 310.

Mobley, C. D. 1994. Light and Water. New York: Academic.

Morel, A. 1991. Optics of marine particles and marine optics. *In* S. Demers [ed.], Particle Analysis in Oceanography. London: Springer Verlag.

Morel, F. M. M., J. G. Reuter, D. M. Anderson, and R. R. L. Guillard. 1979. Aquil: a chemically defined phytoplankton culture medium for trace metal studies. J. Phycol. 15:135-141.

Nelson, N. B., C. A. Carlson, and D. K. Steinberg. 2004. Production of chromophoric dissolved organic matter by Sargasso Sea microbes. Mar. Chem. 89:273-287.

——— and D. A. Siegel. 2002. Chromophoric DOM in the open ocean. *In* D. A. Hansell and C. A. Carlson [eds.], Biogeochemistry of Marine Dissolved Organic Matter. New York: Academic, p. 547-578.

———, D. A. Siegel, C. A. Carlson, C. Swan, W. M. Smethie Jr, and S. Khatiwala. 2007. Hydrography of chromophoric dissolved organic matter in the North Atlantic. Deep-Sea Res. I. 54:710-731.

———, D. A. Siegel, and A. F. Michaels. 1998. Seasonal dynamics of colored dissolved organic material in the Sargasso Sea. Deep Sea Res. I. 45:931-957.

Peacock, T. G., K. L. Carder, P. G. Coble, Z. P. Lee, and S. W. Hawes. 1994. Long-path spectrophotometer for measuring gelbstoff absorption in clear waters. EOS Trans. Am. Geophys. Union. 75:22.

Price, N. M., G. I. Harrison, H. C. Hering, R. J. Hudson, B. Palenik, and F. M. M. Morel. 1989. Preparation and chemistry of the artificial algal culture medium Aquil. Biol. Oceanogr. 6:443-461.

Roesler, C. S., and M. J. Perry. 1995. In situ phytoplankton absorption, fluorescence emission, and particulate backscattering spectra determined from reflectance. J. Geophys. Res. 100(C7):13279-13294.

Siegel, D. A., S. Maritorena, N. B. Nelson, D. A. Hansell, and M. Lorenzi-Kayser. 2002. Global distribution and dynamics of colored dissolved and detrital organic materials. J. Geophys. Res. 107:3228-3241.

Steinberg, D. K., N. B. Nelson, C. A. Carlson, and A. Prusak. 2004. Production of chromophoric dissolved organic matter (CDOM) in the open ocean by zooplankton and the colonial cyanobacterium *Trichodesmium* spp. Mar. Ecol. Prog. Ser. 267:45-56.

Stramski, D., and D. A. Kiefer. 1991. Light scattering by microorganisms in the open ocean. Prog. Oceanogr. 28:343-383.

——— and S. B. Wozniak. 2005. On the role of colloidal particles in light scattering in the ocean. Limnol. Oceanogr. 50:1581-1591.

Twardowski, M. S., E. Boss, J. M. Sullivan, and P. L. Donaghay. 2004. Modeling the spectral shape of absorption by chromophoric dissolved organic matter (CDOM). Mar. Chem. 89:69-88.

———, J. M. Sullivan, P. L. Donaghay, and J. R. V. Zaneveld. 1999. Microscale quantification of the absorption by dissolved and particulate material in coastal waters with an ac-9. J. Atmos. Ocean. Technol. 16:691–707.

Van de Hulst, H. C., 1981, Light Scattering by Small Particles. New York: Dover, 470pp.

Vodacek, A., N. V. Blough, M. D. DeGrandpre, E. T. Peltzer, and R. K. Nelson. 1997. Seasonal variation of CDOM and DOC in the Middle Atlantic Bight: terrestrial inputs and photooxidation. Limnol. Oceanogr. 42:674-686.

Wells, M. L., and E. D. Goldberg. 1991. Occurrence of small colloids in seawater. Nature 353:342-344.